Electrochemical Promotion of Rhodium-Catalyzed NO Reduction by CO and by Propene in the Presence of Oxygen

5 AUTHORS, INCLUDING:

Federico J. Williams
University of Buenos Aires
87 PUBLICATIONS   1,402 CITATIONS

SEE PROFILE

Norman Macleod
Johnson Matthey
24 PUBLICATIONS   773 CITATIONS

SEE PROFILE

Richard Michael Lambert
University of Cambridge
194 PUBLICATIONS   6,729 CITATIONS

SEE PROFILE

Electrochemical Promotion of Rhodium-Catalyzed NO Reduction by CO and by Propene in the Presence of Oxygen

Federico J. Williams, Mintcho S. Tikhov, Alejandra Palermo, Norman Macleod, and Richard M. Lambert*

Department of Chemistry, University of Cambridge, Cambridge CB2 1EW, U.K.

The catalytic performance of a rhodium thin film in contact with the solid electrolyte Na-β'' alumina can be greatly enhanced by the reversible electrochemically controlled transport of sodium from the electrolyte to the metal surface. By this means, the reduction of nitric oxide by carbon monoxide or by propene can be promoted, even in the presence of oxygen. The effect is due to the Na-enhanced dissociation of adsorbed NO, the key reaction-initiating step. XP and Auger spectroscopies show that, under promoted conditions, the alkali-metal surface phase consists of carbonate, nitrate, or both, depending on the gas composition. To a first approximation, the chemical identity of the counterion appears not to play a significant role. With increasing oxygen partial pressure the promotional effects of sodium are progressively decreased, and the markedly different behavior of CO and propene as reductants is due to the opposite effects of coadsorbed alkali metal on the electronegative or electropositive adsorbate, respectively. At the highest oxygen partial pressures and alkali-metal coverages, drastic poisoning by sodium is due to strong alkali-metal inhibition of propene adsorption, excessive formation of Na_2O, and oxidation of Rh to Rh_2O_3.

1. Introduction

The serious environmental implications of NOx emission from automotive sources has stimulated a huge amount of pure and applied research directed at catalytic abatement of such emission. Although so-called three-way catalytic converters are very effective in oxidizing CO and hydrocarbons, they are substantially less effective in reducing NO to nitrogen, producing N_2O in addition.[1] Although nitrous oxide is not yet a regulated pollutant, it is a powerful greenhouse gas, and future legislation is likely to include restrictions on N_2O emission. In this connection, note that over *the warm-up period of the catalyst* N_2O emission accounts for 60−80% of the NO converted by current three-way converters.[2] Another important limitation of three-way converters is that they are ineffective for NO reduction in the presence of excess gaseous oxygen, because O_2 reacts faster with the available reductants than NO itself. This prevents the implementation of fuel-efficient, lean-burn spark ignition engines which would otherwise make a very significant contribution to reduced CO_2 emission. Two important fundamental questions arise. First, how can we improve the selectivity toward N_2 formation? Second, to what extent can any such improvements be sustained in the presence of gaseous oxygen?

We have already shown that alkali-metal additives substantially improve the catalytic activity and nitrogen selectivity of dispersed palladium and platinum catalysts under simulated three-way conditions.[3,4]

In a related effort, we have used electrochemical promotion (EP) to study systematically the effects of alkali-metal modifiers on the catalytic performance of Pt, Cu, and Rh metal film catalysts. EP provides an effective means of studying the effects of promoters and the associated catalytic reaction mechanisms, because it provides in situ control of the promoter concentration at the surface of a working metal catalyst.[5] The technique is implemented by pumping promoter species (Na^+ in the present case) from a suitable solid electrolyte (Na-β'' alumina in the present case) to a porous metal film catalyst with which it is in contact. By varying the catalyst potential (measured with respect to a reference electrode), one may control reversibly the alkali-metal coverage and consequently the catalytic behavior of the metal surface.

Earlier work showed that, in the absence of gaseous oxygen, EP by Na of Rh thin film catalysts greatly enhanced both activity and selectivity toward N_2 production in the reduction of NO by CO[6] and by propene.[7] The resulting insight into the reaction mechanism led to the development of Rh/γ-Al_2O_3 dispersed catalysts, classically promoted by Na, which proved highly efficient in the catalytic reduction of NO by propene.[8] This illustrates the value of EP as a tool for elucidating and exploiting promoter effects in heterogeneous catalysis.

Here, for the first time, we use EP to investigate the effect of added oxygen on alkali-metal promotion of NO reduction. The effects of oxygen partial pressure and catalyst potential (sodium coverage) on the NO + CO + O_2 and NO + C_3H_6 + O_2 reactions have been investigated. Complementary postreaction XPS data were acquired to monitor changes in the amount and chemical identity of the Na compounds present under a variety of conditions, and to determine changes in the oxidation state of the rhodium film.

It is found that sodium does promote both the activity and nitrogen selectivity of rhodium in catalytic reduction of NO by CO or propene, even in the presence of oxygen. Increasing the oxygen partial pressure beyond a certain point decreases the effectiveness of alkali-metal promotion, eventually resulting in a transition to a regime of alkali-metal-induced poisoning. The chemical identity of the alkali-metal surface compounds in the promoted and poisoned regimes is established; the mode of promoter action, the origin of poisoning, and the reaction

* To whom correspondence should be addressed. Phone: 44 1223 336467. Fax: 44 1223 336362. E-mail: rml1@cam.ac.uk.

Electrochemical Promotion of NO Reduction

J. Phys. Chem. B, Vol. 105, No. 14, 2001 **2801**

mechanism are also discussed. The results indicate poisoning due to alkali-metal inhibition of propene adsorption, excessive formation of Na_2O, and oxidation of Rh to Rh_2O_3.

2. Experimental Methods

The EP samples for catalytic testing and spectroscopic analysis were prepared by depositing a rhodium metal film on one face of a Na-β'' alumina wafer: this constituted the catalyst (working electrode). Gold counter and reference electrodes were deposited on the other face, all three electrodes being deposited by dc sputtering of Rh or Au in argon. Methods used for characterizing the Rh film by XRD, XPS, and surface area measurements have been described in detail elsewhere.[6] The true metal area of our rhodium sample was measured by the CO methanation technique described in detail in ref 6.

Reactor measurements were performed in a CST reactor operated at atmospheric pressure. The EP sample was suspended in the reactor with all electrodes exposed to the reactant gas mixture. Inlet and exit gas analysis was carried out by a combination of on-line gas chromatography (Shimadzu-14B; molecular sieves 13X and Haysep-N columns), on-line mass spectrometry (Balzers QMG 064), and on-line nondispersive infrared analyzers (dual channel Siemens Ultramat 6 analyzers calibrated for CO/CO_2 and NO/N_2O). N_2, N_2O, CO, CO_2, O_2, and C_3H_6 were separated and their concentrations determined by gas chromatography; additionally, N_2O, CO, CO_2, and NO were also monitored continuously using the IR detectors after the necessary calibrations were performed. Reaction gases (5% NO/He, 5% CO/He, 5% C_3H_6/He, 20% O_2/He, and He) were of ultrahigh purity and were fed to the reactor by mass flow controllers (Brooks 5850 TR). The total flow rate was kept constant in all experiments at 34×10^{-5} mol s^{-1} (500 cm^3-(STP)/min). Reactant conversion was restricted to <15% to avoid mass-transfer limitations. Control experiments were carried out in which the total flow was varied by a factor of 5 to verify that the observed changes in activity were indeed due to changes in actual surface reaction rates, unaffected by mass-transfer limitations. Nitrogen and carbon mass balances always closed to within 5%. Reactant concentrations are expressed in kPa, where 1 kPa is equivalent to a concentration of 1% or 10000 ppm.

A galvanostat−potentiostat (Ionic Systems) was used to maintain a given potential difference between the working and reference electrodes (potentiostatic mode). All experiments were carried out in potentiostatic mode by following the effect of catalyst potential (V_{WR}, measured with respect to the reference electrode) on the reaction rates.

XPS experiments were performed under UHV conditions (base pressure <10^{-10} Torr) in a VG ADES 400 UHV spectrometer system equipped with a reaction cell. The EP sample was mounted onto a manipulator that allowed translation between the reaction cell and the spectrometer chamber. Full details regarding sample mounting, manipulation, and data acquisition are given in an earlier publication.[9] Quoted binding energies are referred to the Au 4f$_{7/2}$ emission at 83.8 eV from the grounded Au wire that formed the electrical connection to the Rh working electrode. Reference spectra for sodium carbonate and sodium nitrate were obtained by pressing small quantities of the pure compounds into the surface of a pure aluminum disk. This technique gave samples that did not exhibit electrostatic charging effects and were free from carbon contamination.

3. Results

3.1. Effect of Catalyst Potential and Oxygen Concentration on Reaction Rates. *CO as Reductant.* Figure 1 shows typical steady-state (potentiostatic) rate data obtained for the reduction of nitric oxide by carbon monoxide in the presence of oxygen. Turnover frequencies (TOFs) are expressed as molecules of product per Rh surface atom per second. The rates of production of CO_2 (Figure 1a), N_2O (Figure 1b), and N_2 (Figure 1c) at 595 K are shown as a function of catalyst potential (V_{WR}) for constant inlet pressures of NO and CO ($P(CO) = P(NO) = 0.9$ kPa) for a range of oxygen concentration (0, 0.2, 0.4, and 2 kPa). Figure 1d shows the effect of catalyst potential and oxygen concentration on the nitrogen selectivity, where this quantity is defined as the ratio of the nitrogen rate to the sum of the nitrogen + nitrous oxide rates. It is apparent that the CO_2, N_2O, and N_2 reaction rates are dependent on catalyst potential and on the oxygen partial pressure. Decreasing the catalyst potential (*thus increasing the sodium coverage*[5]) in the absence of gaseous oxygen (black circles) increased the rates of CO_2 and N_2 production. In contrast, the rate of formation of N_2O decreased with increasing sodium coverage. As a result, the selectivity toward nitrogen formation increased. As the oxygen partial pressure increased in the interval 0−0.4 kPa, qualitatively similar results were obtained, but with progressive attenuation of the promoting effect of Na. However, at $P(O_2) = 2$ kPa (open circles), the N_2 and N_2O rates (and hence the selectivity) became invariant with Na loading whereas the CO_2 rate showed a small increase at the highest Na loadings. Table 1 summarizes relative rate changes (ratios of maximally promoted/unpromoted reaction rates, ρ) and selectivity variations for the various oxygen concentrations. It should be noted that increasing the oxygen partial pressure causes changes in both the unpromoted ($V_{WR} = +400$ mV) and promoted ($V_{WR} = -300$ mV) conditions. For the unpromoted catalyst, progressively increasing $P(O_2)$ caused (i) increased CO_2 rate, (ii) decreased N_2 rate, (iii) a maximum in the N_2O rate, and (iv) a decrease in the nitrogen selectivity. With the promoted catalyst, increasing $P(O_2)$ caused a progressive decrease in the effect of sodium on (i) reaction rates (all the ρ values tend to unity) and (ii) nitrogen selectivity.

Propene as Reductant. Figure 2 illustrates the effect of sodium and oxygen on the reduction of nitric oxide by propene. The data were obtained at 623 K with $P(C_3H_6) = P(NO) = 1$ kPa and $P(O_2)$ ranging from 0 to 2 kPa. A 1:1 propene:NO ratio was chosen to ensure that the system started out in a regime where the effect of alkali metal is to promote the reaction.[6] Under these conditions of partial pressures and temperature, CO_2, N_2, N_2O, and H_2O were the only products. Parts a−c of Figure 2 show steady-state rate data for CO_2 (a), N_2O (b), and N_2 (c) production as a function of V_{WR} for different (constant) values of oxygen pressure. Figure 2d shows the corresponding nitrogen selectivity data. Decreasing the catalyst potential (*increasing the sodium coverage*) in the absence of gaseous oxygen (filled circles) resulted in the following: (i) increased rates of CO_2 and N_2 formation, (ii) decreased N_2O production, and (iii) a substantial increase in the selectivity toward nitrogen formation. In this respect the behavior is qualitatively similar to that found for CO in the absence of oxygen.

In the presence of gaseous oxygen, electropumping of Na to the catalyst surface in the oxygen pressure range up to 1 kPa again resulted in activity and selectivity promotion. That is, with increased Na loading, the CO_2 and N_2 rates increased, whereas the N_2O rate decreased, resulting in increased nitrogen selectivity. The effects of Na promotion diminished with increasing oxygen partial pressure. However, at $P(O_2) = 2$ kPa, all rates
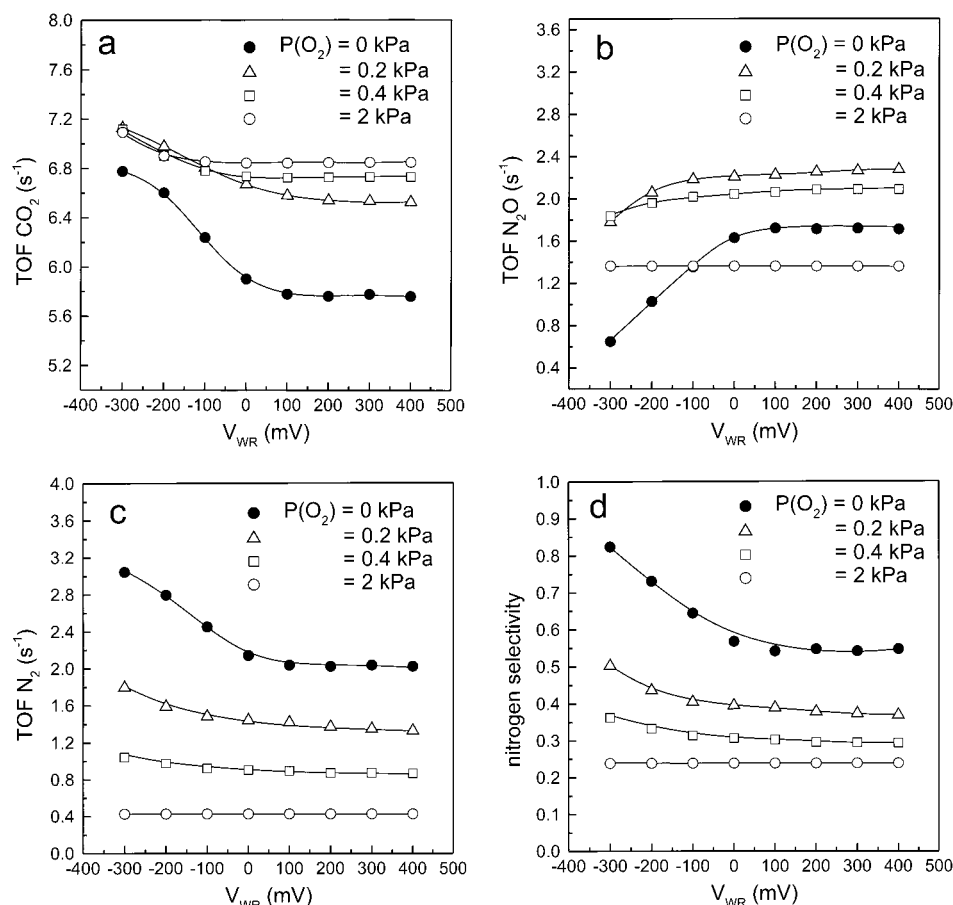
Figure 1. Effect of catalyst potential (V_{WR}) on CO_2 (a), N_2O (b), and N_2 (c) formation rates and on nitrogen selectivity (d) for different partial pressures of oxygen. Conditions: $T = 595$ K, $P(NO) = P(CO) = 0.9$ kPa.

TABLE 1: Effect of Increasing the Oxygen Partial Pressure on the Na-Induced Enhancement of Reaction Rates and Nitrogen Selectivities for the CO + NO Reaction[a]

$P(O_2)$ (kPa)	$\rho(CO_2)$	$\rho(N_2)$	$\rho(N_2O)$	$S^p(N_2)$ (%)
0	1.2	1.5	0.38	54 → 82
0.2	1.1	1.35	0.78	37 → 50
0.4	1.06	1.2	0.88	30 → 36
2	1.03	1	1	24 → 24

[a] u (p) stands for unpromoted (optimally promoted). Conditions: $P(CO) = P(NO) = 0.9$ kPa, $T = 595$ K.

decreased over the accessible range of Na loading, the effect being especially marked in the case of the major products (CO_2, N_2), which no longer exhibited any rate enhancement. In other words, as the oxygen pressure increased the system underwent a switch in behavior. At lower oxygen pressures both reaction rates and nitrogen selectivity were enhanced by Na. However, at 2 kPa of oxygen, pumping Na to the surface resulted in marked activity loss, especially for the nitrogen-containing products, accompanied by a small loss in selectivity. Since this activity loss was so dramatic, the experiment was repeated twice to check the reproducibility. The relevant data are shown as times signs in Figure 2, from which it is evident that (i) the quenching behavior was reproducible and (ii) the electrochemical response was also reversible.

Table 2 shows the effect of sodium on the reaction at different oxygen partial pressures in terms of relative rate changes (ρ) and the corresponding nitrogen selectivity variations. Note that, under unpromoted conditions, progressively increasing the oxygen concentration resulted in a steady increase in the CO_2 rate, whereas the N_2O and N_2 rates and the nitrogen selectivity

passed through a maximum. The general trend is that the promotional effects of sodium on the reduction of NO by CO or propene become less significant as the oxygen partial pressure increases. This abatement of Na promotion is most pronounced when propene is the reductant: in this case the system eventually exhibits total poisoning of catalytic activity when the oxygen exceeds a certain threshold.

To understand these effects of oxygen on catalytic performance, postreaction XPS analyses of the catalyst surface were carried out for the relevant range of oxygen partial pressures and for different catalyst potentials. The results presented refer to the reduction of NO by propene, the more complex of the two systems, because this is the critically important process for practical implementation of catalytic NO reduction in oxygen-containing environments.[10]

3.2. Postreaction XPS Analysis. XP spectra were obtained immediately after the appropriately biased catalyst film was exposed to the conditions of temperature and reactant partial pressures typical of those encountered in the reactor to detect the various surface species present under reaction conditions. During exposure of the catalyst to the reaction mixture, the V_{WR} values were such that the Rh film was either (i) electrochemically clean (unpromoted) or (ii) sodium promoted. A full description of the procedure used to obtain the postreaction XP spectra can be found in an earlier publication.[11]

XP spectra were taken after the sample was exposed to a mixture of 1 kPa of propene + 1 kPa of NO + x kPa of O_2 at 623 K and 1 bar of total pressure (He carrier gas). Here, $x = 0$ kPa, 0.5 kPa (*i.e., conditions under which sodium promotes the reaction*), and 2 kPa (*where sodium poisons the reaction*). The three different reaction mixtures are designated 1, 2, and 3 for
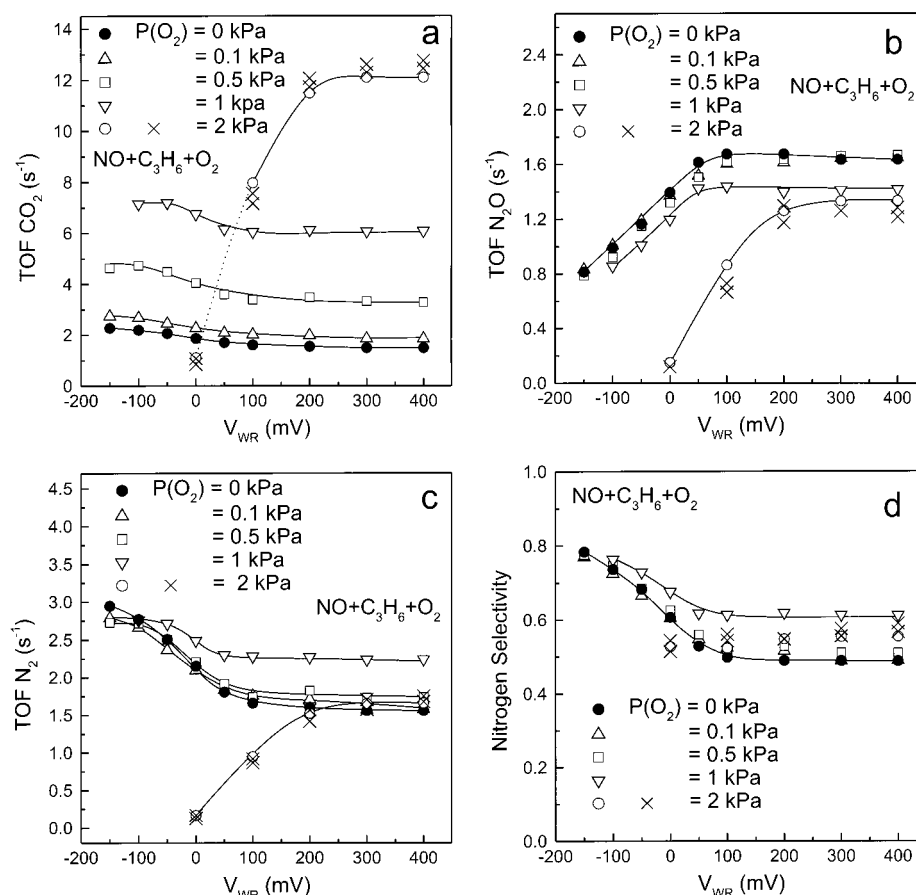
Electrochemical Promotion of NO Reduction

J. Phys. Chem. B, Vol. 105, No. 14, 2001 **2803**

Figure 2. Effect of catalyst potential (V_{WR}) on CO_2 (a), N_2O (b), and N_2 (c) formation rates and on nitrogen selectivity (d) for different partial pressures of oxygen. Conditions: $T = 623$ K, $P(NO) = P(C_3H_6) = 1$ kPa.

TABLE 2: Effect of Increasing the Oxygen Partial Pressure on the Na-Induced Enhancement of Reaction Rates and Nitrogen Selectivities for the C_3H_6 + NO Reaction[a]

$P(O_2)$ (kPa)	$\rho(CO_2)$	$\rho(N_2)$	$\rho(N_2O)$	$S^u(N_2) \rightarrow S^p(N_2)$ (%)
0	1.52	1.89	0.47	49 → 78
0.1	1.47	1.76	0.5	49 → 77
0.5	1.41	1.57	0.47	51 → 77
1	1.17	1.23	0.6	61 → 76
2	0.08	0.07	0.1	55 → 52

[a] u (p) stands for unpromoted (optimally promoted). Conditions: $P(C_3H_6) = P(NO) = 1$ kPa, $T = 623$ K.

$x = 0$, 0.5, and 2.0 kPa of oxygen, respectively. Each reaction gas exposure was carried out for two different values of catalyst potential: (i) $V_{WR} = +600$ mV (*unpromoted catalyst*) and (ii) $V_{WR} = -100$ mV (*promoted catalyst*). XP spectra were thus acquired for the following six sets of conditions:

(1) reaction mixture 1 (without oxygen), unpromoted (spectrum a);

(2) reaction mixture 1 (without oxygen), Na promoted (spectrum b);

(3) reaction mixture 2 ($P(O_2) = 0.5$ kPa), unpromoted (spectrum c);

(4) reaction mixture 2 ($P(O_2) = 0.5$kPa), Na promoted (spectrum d);

(5) reaction mixture 3 ($P(O_2) = 2$ kPa), unpromoted (spectrum e);

(6) reaction mixture 3 ($P(O_2) = 2$ kPa), Na promoted (spectrum f).

Figure 3 shows Na 1s XP spectra for the six different cases described above. It is apparent that a very small amount of

sodium was detectable after the unpromoted sample ($V_{WR} = +600$ mV) was exposed to the different reaction mixtures (spectra a, c, and e). We have shown that this residual emission is from Na in the underlying Na-β'' alumina[5,12] spectroscopically visible through cracks and imperfections present in the porous rhodium film. In every case, electropumping Na to the catalyst ($V_{WR} = -100$ mV) resulted in a substantial increase in Na coverage of the Rh surface (spectra b, d, and f). Note that the binding energy (BE) of the Na 1s XP signal in spectrum f is shifted ~1 eV toward higher BE with respect to spectra b and d. This reflects a change in the nature of the sodium compounds formed in reaction mixture 3.

The top panel in Figure 3 shows Na KLL XAES spectra corresponding to the promoted cases of reaction mixtures 2 and 3, i.e., to XP spectra d and f in the lower panel. (The dashed lines are reference Na KLL spectra for sodium carbonate and sodium nitrate.) These Auger results confirm that the sodium compound present under reaction mixture 3 (spectrum f) is distinct from that present under reaction mixture 2. In addition, they show that the former (spectrum f) is neither a carbonate nor a nitrate, whereas the latter (spectrum d) could be either.

Although the Na 1s BE does depend on the chemical identity of the particular sodium compound (e.g., Na_2CO_3 (1071.5 eV),[13] $NaHCO_3$ (1071.3 eV),[13] $NaNO_2$ (1071.6 eV),[14] $NaNO_3$ (1071.4 eV),[14] Na_2O (1072.5 eV)[15]), this does not provide unambiguous chemical fingerprinting. We therefore identify the various Na compounds by making use of the corresponding C 1s, N 1s, and O 1s spectra. As shown below, the sodium compounds formed may be identified as sodium carbonate (spectrum b), a mixture of sodium carbonate and sodium nitrate (spectrum d), and sodium oxide (spectrum f).
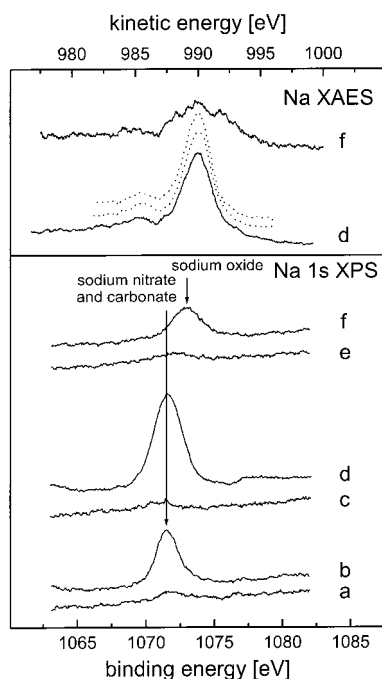
kinetic energy [eV]

Figure 3. Sodium 1s XP spectra acquired after the catalyst was exposed to 1 kPa of propene, 1 kPa of NO, and varying partial pressures of oxygen at $T = 623$ K: $P(O_2) = 0$ kPa, $V_{WR} = +600$ mV (spectrum a) and $V_{WR} = -100$ mV (spectrum b); $P(O_2) = 0.5$ kPa, $V_{WR} = +600$ mV (spectrum c) and $V_{WR} = -100$ mV (spectrum d); $P(O_2) = 2$ kPa, $V_{WR} = +600$ mV (spectrum e) and $V_{WR} = -100$ mV (spectrum f). The top part shows Na KLL XAES spectra corresponding to $P(O_2) = 0.5$ kPa and $V_{WR} = -100$ mV (spectrum d) and $P(O_2) = 2$ kPa and $V_{WR} = -100$ mV (spectrum f). Also shown in dashed lines are the Na KLL reference spectra corresponding to bulk sodium nitrate and carbonate samples.
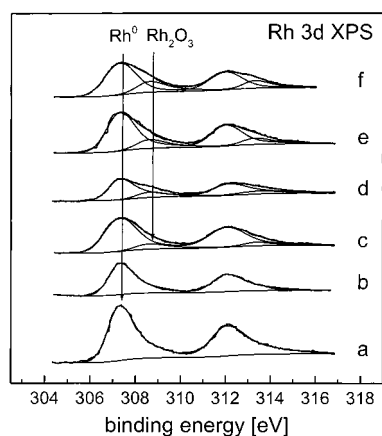

Figure 4. Rhodium 3d XP spectra acquired after the catalyst was exposed to 1 kPa of propene, 1 kPa of NO, and varying partial pressures of oxygen at $T = 623$ K: $P(O_2) = 0$ kPa, $V_{WR} = +600$ mV (spectrum a) and $V_{WR} = -100$ mV (spectrum b); $P(O_2) = 0.5$ kPa, $V_{WR} = +600$ mV (spectrum c) and $V_{WR} = -100$ mV (spectrum d); $P(O_2) = 2$ kPa, $V_{WR} = +600$ mV (spectrum e) and $V_{WR} = -100$ mV (spectrum f).

Rh 3d XP spectra are shown in Figure 4. Note that under our conditions the inelastic mean free path of the Rh photoelectrons (kinetic energy 946 eV) was ∼11 Å,[16] which provides the required surface sensitivity. These data illustrate two important points. First, the BE shifts indicate changes in the oxidation state of the rhodium film. Second, in any given case, the intensity attenuation provides a measure of the coverage of the metal by surface species. Two main contributions may be distinguished in the Rh 3d spectra: the lower BE doublet at 307.3 and 312 eV corresponds to metallic rhodium, whereas

TABLE 3: Effect of Increasing Oxygen Partial Pressure and Na Coverage on the Oxidation of the Rh Catalyst and on the Attenuation of the Rh 3d XPS Signal for the C_3H_6 + NO + O_2 Reaction[a] Conditions: $P(C_3H_6) = P(NO) = 1KPa$, T=623K

$P(O_2)$ (kPa)	V_{WR} (mV)	oxidation (%)	attenuation (%)	film thickness (Å)
0 (spectrum a)	+600	0	13	1.3
0 (spectrum b)	−100	0	53	7
0.5 (spectrum c)	+600	14	38	4.6
0.5 (spectrum d)	−100	21	58	8.3
2 (spectrum e)	+600	23	36	4.3
2 (spectrum f)	−100	30	42	5.2

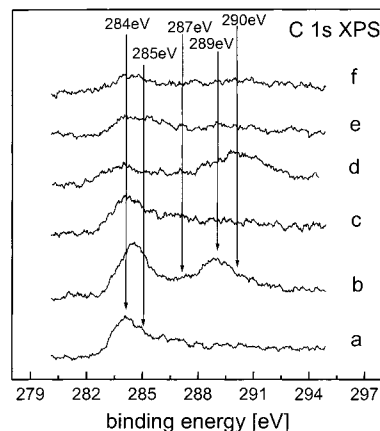[a] Conditions: $P(C_3H_6) = P(NO) = 1$ kPa, $T = 623$ K.

Figure 5. Carbon 1s XP spectra acquired after the catalyst was exposed to 1 kPa of propene, 1 kPa of NO, and varying partial pressures of oxygen at $T = 623$ K: $P(O_2) = 0$ kPa, $V_{WR} = +600$ mV (spectrum a) and $V_{WR} = -100$ mV (spectrum b); $P(O_2) = 0.5$ kPa, $V_{WR} = +600$ mV (spectrum c) and $V_{WR} = -100$ mV (spectrum d); $P(O_2) = 2$ kPa, $V_{WR} = +600$ mV (spectrum e) and $V_{WR} = -100$ mV (spectrum f).

the higher BE doublet at 308.6 and 313.3 eV is due to Rh_2O_3.[17] Within the XPS sampling depth, the fraction of the catalyst that had undergone oxidation under the reaction conditions can be estimated from the ratio of the integrated intensity corresponding to the Rh_2O_3 to the total integrated intensity. The results of this procedure are given in Table 3, which interprets the attenuation of Rh 3d emission in terms of the effective thickness of a hypothetical continuous film of overlying material. The first entry (1.3 Å) is of course physically unrealistic and is best thought of as equivalent to ∼1/3 of a monolayer of adsorbate on an otherwise bare Rh surface. It is evident from Table 3 that coverage of the postreaction Rh catalyst by surface species is greater under promoted than unpromoted conditions. The results in Table 3 also show that the rhodium film undergoes oxidation only when there is O_2 present in the gas phase. It is also evident that the degree of oxidation of the rhodium film increased with (i) the oxygen partial pressure and (ii) Na loading.

Figure 5 shows carbon 1s XP spectra for the six different conditions described above. These provide some information about the chemical identity of the Na compounds that are formed under reaction conditions. The C 1s region exhibits two main contributions, one at lower binding energy (∼284−285 eV) and the other at higher binding energy (∼288−290 eV). The former is due to elemental carbon (284 eV[18]) and to propene fragments (284−285 eV), whereas the latter is due to sodium carbonate (289 eV[19]). The small feature at ∼287 eV could be due to partially oxidized carbonaceous species.[18] After the catalysts were exposed to reaction mixture 1 under unpromoted conditions (spectrum a), at least two peaks were apparent due to (i) elemental carbon and (ii) propene fragments. Exposing the
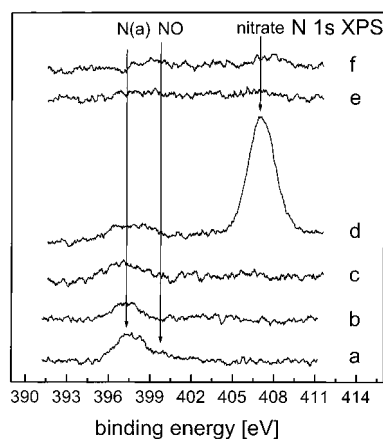
Electrochemical Promotion of NO Reduction

J. Phys. Chem. B, Vol. 105, No. 14, 2001 **2805**

Figure 6. Nitrogen 1s XP spectra acquired after the catalyst was exposed to 1 kPa of propene, 1 kPa of NO, and varying partial pressures of oxygen at $T = 623$ K: $P(O_2) = 0$ kPa, $V_{WR} = +600$ mV (spectrum a) and $V_{WR} = -100$ mV (spectrum b); $P(O_2) = 0.5$ kPa, $V_{WR} = +600$ mV (spectrum c) and $V_{WR} = -100$ mV (spectrum d); $P(O_2) = 2$ kPa, $V_{WR} = +600$ mV (spectrum e) and $V_{WR} = -100$ mV (spectrum f).
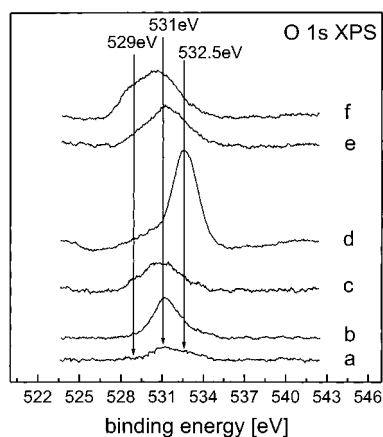

Figure 7. Oxygen 1s XP spectra acquired after the catalyst was exposed to 1 kPa of propene, 1 kPa of NO, and varying partial pressures of oxygen at $T = 623$ K: $P(O_2) = 0$ kPa, $V_{WR} = +600$ mV (spectrum a) and $V_{WR} = -100$ mV (spectrum b); $P(O_2) = 0.5$ kPa, $V_{WR} = +600$ mV (spectrum c) and $V_{WR} = -100$ mV (spectrum d); $P(O_2) = 2$ kPa, $V_{WR} = +600$ mV (spectrum e) and $V_{WR} = -100$ mV (spectrum f).

catalyst to reaction mixture 1 under promoted conditions (spectrum b) generated at least four C 1s contributions, namely, (i) elemental carbon, (ii) propene fragments, (iii) a shoulder at 287.4 eV, possibly due to partially oxidized carbonaceous species, as noted above, and (iv) a peak at 289 eV due to sodium carbonate. Progressive addition of oxygen to the reaction gas resulted in a corresponding decrease in the amount of elemental carbon and carbonaceous species (spectra c−f). The emission at 289−290 eV due to sodium carbonate persists in spectrum d (reaction mixture 2, promoted conditions) but is eventually quenched (spectra f corresponding to reaction mixture 3, promoted conditions). Note that the peak ascribed to carbonate is upshifted by ∼1 eV between spectrum b and spectrum d. In summary, (i) the presence of gaseous oxygen decreases coverage by carbon and carbonaceous species, (ii) carbonate is only present when the catalyst exhibits promotion by Na, and (iii) carbonate is absent when the catalyst exhibits poisoning by Na.

Figure 6 shows corresponding N 1s XP spectra in which two contributions are readily apparent: chemisorbed N at 397.4 eV[20] and nitrate at 407.3 eV.[21] In addition, spectrum a exhibits a weak feature at 400 eV that may be ascribed to chemisorbed NO.[22] Thus, exposure to reaction mixture 1 under unpromoted conditions results in the presence of both chemisorbed N and NO (spectrum a), whereas under promoted conditions only chemisorbed N is detected (spectrum b). When the reaction gas contains some oxygen (reaction mixture 2), only chemisorbed N is detected on the unpromoted surface (spectrum c). However, Na promotion in reaction mixture 2 generates both N adatoms and nitrate (spectrum d). At the highest oxygen pressure (reaction mixture 3) no nitrogen-containing adsorbates are detectable on both the unpromoted and promoted surfaces (spectra e and f).

The O 1s XP spectra shown in Figure 7 contain three principal contributions. The lowest BE peak (529−530 eV) is due to rhodium oxide (530 eV[17]) and Na_2O (529.6 eV[15]). The 531.4 eV BE peak is due to chemisorbed oxygen[17] and carbonate (531.6 eV[23]). The highest BE peak (532.5 eV) must be associated with a sodium compound since it disappears upon imposing a positive bias (thus pumping Na away from the Rh surface). We therefore assign it to sodium nitrate, in good agreement with the reported BE for this compound[24] and the corresponding N 1s spectrum shown in Figure 6. It is possible that subsurface oxygen may make a small contribution at this

BE.[17] Exposure of the unpromoted surface to oxygen-free reaction gas (mixture 1) under unpromoted conditions generates chemisorbed oxygen and subsurface oxygen (spectrum a). Alkali-metal promotion in the same reaction gas (mixture 1) produces chemisorbed oxygen, sodium carbonate (cf. the C 1s spectrum b), and subsurface oxygen. Addition of oxygen (mixtures 2 and 3) results in the appearance of an emission at 530 eV that correlates with the oxidation of the rhodium film detected in the Rh 3d spectra (Figure 4). Accordingly, this O 1s emission is assigned to Rh_2O_3. Specifically, exposing the unpromoted surface to the oxygen-containing reaction mixture 2 produced rhodium oxide and chemisorbed oxygen (spectrum c); Na promotion in the same reaction gas produced Na nitrate in addition to Rh_2O_3 and O(a) (spectrum d). At the highest oxygen pressure (reaction mixture 3) rhodium oxide and chemisorbed oxygen are again present in the unpromoted conditions (spectrum e). This time, however, Na pumping to the catalyst resulted in *poisoning*, and the appearance of Na_2O rather than $NaNO_3$ (spectrum f).

It is worth noting that in every case application of $V_{WR} = +600$ mV at reaction temperature (pumping Na away from the catalyst) resulted in complete disappearance of the sodium compounds (variously carbonate, nitrate, and oxide), leaving only a small amount of chemisorbed oxygen on the Rh surface. This provides confirmation of the overall validity of the spectral interpretations offered above, and the conclusions drawn on the catalytic behavior, proposed below.

4. Discussion

Interpretation of our reactor data requires the explanation of two principal phenomena. First, there is a regime in which increasing the sodium coverage causes an increase in reaction rates and nitrogen selectivity. Second, as the oxygen content in the gas phase is increased the effects of sodium promotion on the nitrogen rate and selectivity progressively decrease. The effect is most pronounced in the case of the NO + propene reaction, where all promotional effects are eventually suppressed and the system actually exhibits total poisoning of all catalytic activity. However, before the effects of electrochemically supplied sodium are discussed, it is necessary to consider the chemical state of the promoter phase under reaction conditions.

4.1. Chemical State of the Alkali-Metal Additive under Reaction Conditions. The postreaction XPS demonstrates that

the chemical identity of the sodium-containing promoting (or poisoning) phases is dependent on the gas atmosphere. When the gas phase consisted of equal amounts of NO and propene (spectra b), sodium was present as the carbonate. Addition of some oxygen (spectra d) resulted in a mixture of sodium carbonate and nitrate being formed. Ultimately, at the highest oxygen pressure (spectra f) sodium oxide was formed. Our results indicate that the identity of the adsorbed counterion(s) (nitrate, carbonate) is not critically important in determining the promoting effect of Na. This effect has been discussed elsewhere[4] within the theoretical framework developed by Lang et al.[27]
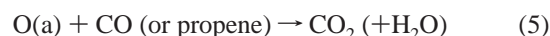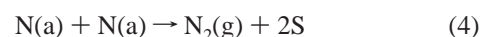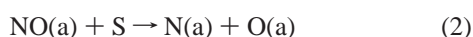
The Rh 3d XP spectra (Figure 4) are revealing in regard to the extent of loading and morphology of the Na surface compounds. Under promoted conditions the Rh XP signal is attenuated by an overlayer consisting principally of sodium compounds. Since this surface is catalytically active, at least some of the surface must expose promoter-modified Rh sites while the rest is covered by the Na compound. Therefore, the nominal film thickness values given in Table 3 (7, 8.3, and 5.2 Å) imply that under promoted conditions the sodium compounds are present, at least in part, as three-dimensional crystallites. The peaks at 289 and 290 eV in the C 1s XP spectra (Figure 5, spectra b and d) have been assigned to sodium carbonate. This assignment is based on our own reference spectrum (BE = 289.5 eV) and on values reported in the literature. These latter range from 289.4 eV for bulk sodium carbonate samples[25] to 290.4 eV for submonolayer quantities of sodium carbonate.[26] Therefore, we propose that the BE variations we observe reflect a change in the state of aggregation of the sodium carbonate from largely three-dimensional to mainly two-dimensional.

4.2. Mode of Alkali-Metal Promotion. The reactor data clearly demonstrate the reversible dependence of reaction rates on catalyst potential. This is due to the reversible, potential-controlled, electropumping of sodium ions from the solid electrolyte to the rhodium catalyst. Equally, the postreaction XPS data (Figure 3) show the occurrence of reversible spillover/back-spillover of Na to/from the surface of the Rh film. Decreasing the catalyst potential delivers Na to the surface, which, in the presence of a reactive gas atmosphere, results in the formation of sodium compounds whose chemical identity depends on the composition of the gas phase. The resulting promotional effects of sodium on the reduction of NO by CO or propene may be understood in terms of the enhanced NO adsorption and dissociation induced by the coadsorbed Na^+. The dissociation of adsorbed diatomic molecules in the electric field of adjacent alkali-metal cations has received a detailed theoretical analysis[27] and may be regarded as well understood. The field lowers the energy of the NO antibonding orbital with respect to the Fermi level, thus increasing charge transfer from Rh to the NO π^* orbital, resulting in increased metal–N bond strength and decreased N–O bond strength. Clear experimental evidence for alkali-metal-induced NO dissociation comes from single-crystal studies on Rh(111)/K[28,29] and on Rh(100)/Na.[30]

On the above basis, the following reaction mechanism permits a rationalization of promotion by Na of the Rh-catalyzed reduction of NO by CO or propene in the absence of oxygen. The mechanism is also consistent with the single-crystal studies of Belton et al.[31]

$$NO(g) + S \rightarrow NO(a) \qquad (1)$$
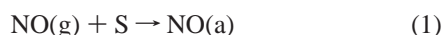
S represents a vacant site for adsorption. Oxygen adatoms

$$NO(a) + S \rightarrow N(a) + O(a) \qquad (2)$$

$$NO(a) + N(a) \rightarrow N_2O(g) + 2S \qquad (3)$$

$$N(a) + N(a) \rightarrow N_2(g) + 2S \qquad (4)$$

$$O(a) + CO \text{ (or propene)} \rightarrow CO_2 \text{ } (+H_2O) \qquad (5)$$

produced in the critical reaction-initiating step (2) react with adsorbed CO (or with hydrocarbon fragments, in the case of propene) to form CO_2. *In this scheme, (2) is rate limiting[31]* and is promoted by Na as argued above. Nitrogen selectivity depends on the relative rates of (3) and (4). Na promotes activity and nitrogen selectivity as a result of accelerating (2), increasing N(a) and O(a) coverages and decreasing that of NO(a). As a result, there is an increase in the rates of N_2 and CO_2 production in (4) and (5), respectively, and a decrease in the rate of (3), yielding the observed increase in overall activity and nitrogen selectivity (Figures 1 and 2).

Consider now the effects of added oxygen. Figure 1 shows that, in the case of the NO + CO reaction, increasing the oxygen partial pressure *in the absence of Na promotion* causes (i) an increase in the CO_2 production rate, (ii) a decrease in the rate of N_2 production, (iii) a maximum in the rate of N_2O production, and (iii) a decrease in nitrogen selectivity. These effects can be understood in terms of the competitive adsorption of oxygen and NO. Increasing the oxygen partial pressure causes an increase in the oxygen coverage, resulting in an increase in the CO_2 rate as observed. At the same time NO adsorption and dissociation are inhibited, resulting in a decrease in both the nitrogen rate and nitrogen selectivity. The maximum in the unpromoted N_2O rate as a function of increasing oxygen content may be understood as follows. When $P(O_2) = 0$, the N_2O rate is low (see Figure 1b) because NO dissociation is efficient. However, as the O_2 pressure increases to 0.2 kPa, N_2O production increases because increased O(a) coverage inhibits NO dissociation, thus increasing θ_{NO} and favoring N_2O formation. A further increase in $P(O_2)$ decreases N_2O production due to decreased NO adsorption resulting from increased competition from O_2 for vacant sites.

The behavior observed with propene as reductant is similar, though not indentical. As shown in Figure 2, increasing the oxygen pressure in the absence of Na results in (i) an increase in the CO_2 rate and (ii) the rate of nitrogen production and the nitrogen selectivity passing through a maximum. These effects may be rationalized as follows. Spectrum a in Figure 5 shows that in the absence of gaseous oxygen the surface of the catalyst is covered mainly by hydrocarbon fragments. Increasing the oxygen partial pressure results in an increase in oxygen coverage, "cleaning off" hydrocarbonaceous fragments (also shown in Figure 5), and thus increasing the rate of CO_2 production. As a result, the number of free sites available for NO adsorption and dissociation increases, resulting in an increase in the rate of nitrogen production and in nitrogen selectivity. However, a further increase in oxygen partial pressure eventually leads to a decrease in site availability for NO dissociation as the surface becomes overpopulated by O(a). Therefore, the nitrogen rate and nitrogen selectivity should both fall, so that the maximum exhibited by both these quantities is understandable.

4.2. Oxygen-Induced Inhibition of Alkali-Metal Promotion. Here we discuss the consequences of increasing the oxygen partial pressure under *promoted* conditions. As shown in Figures 1 and 2, the promotional effects of sodium on the reduction of NO by both CO and propene decrease as the oxygen partial pressure is increased. This occurs to the extent that they

Electrochemical Promotion of NO Reduction

J. Phys. Chem. B, Vol. 105, No. 14, 2001 **2807**

disappear (when CO is used as the reductant) or they result in a decrease in reaction rates (when propene is used as the reductant) when oxygen is increased above a certain threshold. This behavior is explicable in terms of the effect of alkali-metal modifiers on the competitive adsorption of the reactants. Sodium is an electropositive adsorbate and should therefore decrease the strength of chemisorption of electron-donating adsorbates (propene); conversely, it should strengthen the chemisorption of electron acceptors (CO, NO, and O(a)). The postreaction XP data are in accord with this view: spectra c, d, e, and f in Figures 5 and 7 show that sodium increases the steady-state coverage of oxygen-containing species at the expense of adsorbed hydrocarbon fragments.

Thus, progressive suppression of the promoting effect of sodium promotion by addition of gaseous oxygen is due to alkali-metal-enhanced adsorption of oxygen at the expense of propene: the system self-poisons by excessive adsorption of one of the reactants. The other consequence of alkali-metal-enhanced oxygen adsorption is oxidation of the rhodium catalyst itself (Figure 4). Alkali-metal-enhanced oxidation of silicon is well-known[32] and has recently been reported in the case of copper.[11]

It is known that sodium enhances the adsorption and dissociation of CO, NO, and O_2 when coadsorbed separately with these species on rhodium.[30] However, the effect of sodium on the competitive adsorption of CO, NO, and O_2 is not known. Our data show that the unpromoted rate of nitrogen production decreases as the partial pressure of oxygen increases. As discussed above, this implies decreased NO adsorption and dissociation resulting from increased competition from O_2 for vacant sites. In the Na-promoted case the nitrogen rate also decreases as $P(O_2)$ increases. This suggests that sodium enhances oxygen adsorption more strongly than that of nitric oxide. As a consequence, increasing $P(O_2)$ under promoted conditions results in a relative increase of the surface coverage of oxygen adatoms at the expense of both free sites and NO molecules, thus resulting in a decrease in the level of promotion. That is, alkali-metal-enhanced NO dissociation diminishes as $P(O_2)$ increases because the probability of NO(a) interacting with a Na-promoted Rh site decreases as O(a) increases.

Why is oxygen inhibition of alkali-metal promotion more pronounced in the case of propene (where actual poisoning is observed) than in the case of CO? With CO as reductant, adding O_2 decreased the promotional effects of sodium. As discussed above, this is due to the decreased probability of NO(a) interacting with a Na-promoted Rh site as O(a) increases. However, with propene as the reductant, at the maximum oxygen pressure, adding sodium actually poisoned all reactions. This difference in behavior is understandable in terms of the opposite effects of sodium on the chemisorption of the two reductants. Thus, sodium enhances the adsorption of CO, whereas it *decreases* the adsorption strength of propene. As a result, at sufficiently high oxygen pressure, the propene + NO reaction is strongly inhibited by two effects that work in the same direction: alkali-metal-enhanced NO dissociation is suppressed, and propene adsorption is also suppressed. With CO the second effect does not occur: although sodium stops promoting NO dissociation, it still promotes the oxidation of carbon monoxide (reflecting the alkali-metal-enhanced adsorption of both CO and oxygen).

It is worth noting that the behavior of this EP system closely parallels that found with classically promoted conventional dispersed catalysts. Thus, Macleod et al. found that although sodium promotes the reduction of NO by propene over Rh/γ-

alumina catalysts,[8] it actually poisons the system under three-way conditions,[33] i.e., in the presence of substantial amounts of gaseous oxygen. This provides further support for the view that EP studies on model thin film catalysts provide insight into the behavior of the corresponding practical dispersed catalysts.

5. Conclusions

(1) Electrochemically supplied sodium can promote both the catalytic activity and nitrogen selectivity in the rhodium-catalyzed reduction of NO by CO or propene, even in the presence of oxygen. This is understandable in terms of alkali-metal-enhanced NO chemisorption and dissociation.

(2) Under promoted conditions, the alkali-metal surface phase consists of carbonate, nitrate, or both, depending on the gas composition. To a first approximation the chemical identity of the counteranion appears not to play a significant role. Some of this material is present as three-dimensional crystallites.

(3) With increasing oxygen partial pressure the promotional effects of sodium are progressively decreased. This is understandable in terms of alkali-metal-enhanced adsorption of oxygen and subsequent suppression of NO adsorption and dissociation.

(4) With propene as reductant, actual poisoning by sodium occurs at the highest oxygen partial pressure and is due to three additional effects, namely, strong alkali-metal inhibition of propene adsorption, excessive formation of Na_2O, and oxidation of Rh to Rh_2O_3.

(5) The markedly different behavior of CO and propene as reductants is due to the opposite effects of coadsorbed alkali metal on the electronegative or electropositive adsorbate, respectively.

References and Notes

(1) Taylor, K. C. *Catal. Rev. Sci. Eng.* **1993**, *35*, 457.

(2) Cant, N. W.; Angove, D. E.; Chambers, D. C. *Appl. Catal., B* **1998**, *17*, 63.

(3) MacLeod, N.; Issac, J.; Lambert, R. M *J. Catal.*, in press.

(4) Konsolakis, M.; MacLeod, N.; Issac, J.; Yentekakis, I. V.; Lambert, R. M *J. Catal.* **2000**, *193*, 330.

(5) Williams, F. J.; Palermo, A.; Tikhov, M. S.; Lambert, R. M. *J. Phys. Chem. B* **2000,** *104,* 615.

(6) Williams, F. J.; Palermo, A.; Tikhov, M. S.; Lambert, R. M. *J. Phys. Chem. B* **2000,** *104*, 11883.

(7) Williams, F. J.; Palermo, A.; Tikhov, M. S.; Lambert, R. M. *J. Phys. Chem. B*, in press.

(8) Macleod, N.; Isacc, J.; Lambert, R. M. *J. Catal.* **2000**, *193*, 115.

(9) Lambert, R. M.; Williams, F. J.; Palermo, A.; Tikhov, M. S. *Top. Catal.* **2000**, *13,* 91.

(10) Burch, R.; Millington, P. J.; Walker, A. P. *Appl. Catal., B* **1994**, *4*, 65.

(11) Williams, F. J.; Palermo, A.; Tikhov, M. S.; Lambert, R. M. *J. Phys. Chem. B* **1999**, *103,* 9960.

(12) Yentekakis, I. V.; Palermo, A.; Filkin, N. C.; Tikhov, M. S.; Lambert, R. M. *J. Phys. Chem. B* **1997**, *101*, 3759.

(13) Wagner, C. D.; Riggs, W. M.; Davis, L. E.; Moulder, J. F.; Muilenberg, G. E. *Handbook of X-ray Photoelectron Spectroscopy*; Perkin-Elmer Corporation, Physical Electronics Division: Eden Prairie, MN, 1979.

(14) Wagner, C. D. *Discuss. Faraday Soc.* **1975**, *60*, 291.

(15) Barrie, A.; Street, F. J. *J. Electron Spectrosc. Relat. Phenom.* **1975**, *7*, 1.

(16) Penn, D. R. *J. Electron Spectrosc. Relat. Phenom.* **1976**, *9*, 29.

(17) Tolia, A. A.; Smiley, R. J.; Delgass, W. N.; Takoudis, C. G.; Weaver, M. J. *J. Catal.* **1994**, *150*, 56.

2808 *J. Phys. Chem. B, Vol. 105, No. 14, 2001*

Williams et al.

(18) Paal, Z.; Schlogl, R.; Ertl, G. *J. Chem. Soc., Faraday Trans.* **1992**, *88*, 1179 and references therein.

(19) Seyller, Th.; Borgmann, D.; Wedler, G. *Surf. Sci.* **1998**, *400*, 63.

(20) Baird, R. J.; Ku, R. C.; Wynblatt, P. *Surf. Sci.* **1980**, *97*, 346.

(21) Folkesson, B. *Acta Chem. Scand.* **1973**, *27*, 287.

(22) DeLouise, L. A.; Winograd, N. *Surf. Sci.* **1985**, *159*, 199.

(23) Wagner, C. D.; Zatko, D. A.; Raymond, R. H. *Anal. Chem.* **1980**, *52*, 1445.

(24) Bandis, C.; Scudiero, L.; Langford, S. C.; Dickinson, J. T. *Surf. Sci.* **1999**, *442*, 413.

(25) Gelius, U.; Heden, P. F.; Hedman, J.; Lindberg, B. J.; Manne, R.; Nordberg, R.; Nordling, C.; Siegbahn, K. *Phys. Scr.* **1970**, *2*, 70.

(26) Nerlov, J.; Christensen, S. V.; Weichel, S.; Pedersen, E. H.; Moller, P. J. *Surf. Sci.* **1997**, *371*, 321.

(27) Lang, N. D.; Holloway, S.; Norskov, J. K. *Surf. Sci.* **1985**, *150*, 24.

(28) Bugyi, L.; Solymosi, F. *Surf. Sci.* **1987**, *188*, 475.

(29) Bugyi, L.; Kiss, J.; Revesz, K.; Solymosi, F. *Surf. Sci.* **1990**, *233*, 1.

(30) Hochst H.; Colavita, E. *J. Vac. Sci. Technol., A* **1986**, *4*, 1442.

(31) Herman, G. S.; Peden C. H. F.; Schmieg, S. J.; Belton, D. N. *Catal. Lett.* **1999**, *62*, 131 and references therein.

(32) Riehlchudoba, M.; Schirm, K. M.; Surnev, L.; Soukiassian, P. *Surf. Sci.* **1995**, *333*, 375.

(33) MacLeod, N.; Issac, J.; Lambert, R. M. *Appl. Catal. B*, submitted for publication.